Journal of Rehabilitation in Civil Engineering 8-3 (2020) 124-138

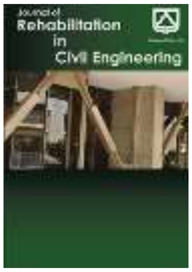


Journal homepage: http://civiljournal.semnan.ac.ir/

# Numerical Investigation of Composite Shear Walls with Different Types of Steel and Concrete Materials as Boundary Elements

**A. Kheyroddin[1*], M. Hajforoush [1] and A. Doustmohammadi [1]**

1. Department of Civil Engineering, Semnan University, Semnan, Iran.

Corresponding author: *kheyroddin@semnan.ac.ir*

**ARTICLE INFO**

Article history:
Received: 28 May 2019
Accepted: 08 April 2020

**Keywords:**
Boundary element,
Composite shear wall,
Numerical analysis,
Seismic-resistant structural system.

**ABSTRACT**

The main purpose of this study is to numerically assess the effect of boundary elements with different types of steel and concrete materials on nonlinear performance of composite steel–reinforced concrete wall (CSRCW) by employing ABAQUS software. Two types of common steel profiles including box and I-shaped sections, located at the middle and extremities of the wall, were used to assess ultimate strength of the CSRCW. In addition, effects of concrete confinement on boundary elements were investigated for fully and partially encasement degrees. Following this, steel materials with three yield stresses of 300, 400 and 500 MPa, and concrete in two grades with compressive strengths of 30 and 40 MPa were considered. The theoretical results demonstrated that numerical models can predict the fracture zones similar to experimental observations where the failure modes of CSRCWs appeared to have ductile mechanisms. Based on the numerical outputs, the presence of I-shaped steel section in the middle of CSRCW participated to effectively distribute the stress throughout the shear wall, which was found to be 6.5% higher than that conventional shear wall. Furthermore, using steel boundary elements with higher yield strengths caused the highest amount of ultimate strength for the CSRCW to be 397.1 kN.

## 1. Introduction

To achieve the intended lateral strength and stiffness of structures, some composite steel–concrete structural systems have been proposed by researchers [1-4]. Among these systems, composite steel-reinforced concrete wall (CSRCW) as a suitable lateral load-

DOI: 10.22075/JRCE.2020.17929.1343

resisting system has been suggested to withstand seismic loads. The CSRCWs are comprised of reinforced concrete (RC) wall with additional structural steel, located at the extremities of the cross section of the wall, and also shear studs which are used to provide the composite action [5-8]. This system has the ability to induce a good flexural stiffness and an adequate ductility compared to conventional reinforced concrete shear walls [9]. Meanwhile, the addition of high strength steel and pozzolanic materials to concrete can enhance its energy dissipation capacity [10,13]. Nonlinear behavior of different types of composite shear walls have been investigated by many researches. Following this, Guan et al. [14] investigated the effect of ring stirrups as concrete filled steel tubes on the behavior of composite shear walls. They showed that the ring stirrups can efficiently prevent the collapse of the wall subjected to axial loads. In addition, Tuppor [15] evaluated the hysteretic behavior of RC walls with steel boundary elements. He reported that the seismic responses of the walls with boundary elements are very nearly to that of conventional RC flexural wall. Zhao et al. [16] and also Zhang et al. [17] investigated the monotonic and cyclic behaviors of encased steel plate reinforced gangue concrete composite shear wall. They concluded that the load-carrying capacity of the wall is developed as the axial compression ratio and steel plate strength increased. While, increasing the height-width ratio can decrease it. Teng Huang et al. [18] suggested a concrete filled double skin steel plate composite wall, and concluded that the proposed system has a great energy dissipation capacity in comparison with conventional shear walls. A study performed by Rassouli et al. [19] showed that the infill steel plate resists inelastic deformations through large lateral displacements. Kheyroddin and Mirza [20,21] proposed a new equation for estimating of flexural rigidity, EI, for RC flexural members. They reported that compressive strength of concrete and compression reinforcement ratio have a remarkable effect on EI values for heavily reinforced flexural members. This effect is reduced with a decrease in the tension reinforcement ratio. At the same level of moment, the flexural rigidity of beams loaded at the mid span was found to be 18% more than that for beams under uniformly distributed load. Ayazi and Shafaei [22] evaluated the effect of high performance fiber reinforced concrete panels on steel–concrete composite shear walls. They indicated that the use of the panels causes an increase in the ductility ratio of the system. Dan et al. [23] investigated the performance of CSRCW with steel encased profiles. The results demonstrated that CSRCWs have a great plastic resistance to compression in comparison with concrete shear walls. The stiffness value also increased as the amount of steel increased. Stoian et al. [24] and also Sun et al. [25] showed that ductile failure being experienced by the tested elements for the CSRCWs.

The performance of shear studs in the CSRCW was assessed by Saari et al. [26]. They found that the ultimate strength and deformation capacity of the studs can be used to provide confinement effects. Hossain and Wright [27] suggested a new form of composite walling system consisted of two skins of steel sheeting with an in-fill of concrete. They concluded that the adequate connections can increase the shear resistance of the wall. Tong et al. [28] assessed the hysteretic performance of steel frame structures with composite RC in-fill walls and partially-restrained connections. Concerning this, the RC in-fill wall exhibits approximately uniform shear deformation. Furthermore, the system showed to have an appropriate strength for withstanding lateral loads like earthquake, and a sufficient stiffness for controlling drift ratio. Rahnavard et al. [29] numerically assessed the influence of significant parameters such as distance between connectors and concrete cover on the behavior of the CSRCW. They reported that the lateral stiffness of the CSRCW is not affected by changing the concrete cover thickness and distance between connectors. Following this, the seismic behavior of the CSRCW with vertical steel encased profiles was evaluated by Dan et al. [30]. Increasing stirrups can decrease the local crushing of concrete under compression. Furthermore, the connectors can increase the anchorage of steel profiles, and avoid the splitting of concrete.

The seismic performance of composite steel plate shear walls was evaluated by Astaneh [31]. The results demonstrated that the adequate boundary members are required for creating openings in the wall. In addition, headed shear studs should be employed to prevent local buckling of the steel plate. According to the results given by Epackachi [32], steel plate shear wall buckling is decreased by increasing concrete cover thickness, and by decreasing distance between connectors.

For the purpose of further investigation on the effect of boundary elements on the seismic performance of CSRCWs, the behavior of CSRCW was numerically assessed considering steel materials with three different yield stresses: 300 MPa, 400 MPa and 500 MPa. The study also investigated, the effect of concrete with two different compressive strengths: 30 and 40 MPa on the numerical modeling of CSRCW.

## 2. Material Properties and Details of Numerical Models

In the present study, the experimental results of Dan et al. [30] were used to verify numerical modeling. Six specimens of the CSRCW were investigated by Dan et al. [30] as detailed in Table 1. Properties of steel and concrete materials are presented in Tables 2 and 3, respectively. The modulus of elasticity of concrete is calculated using Eq. (1) as presented by Hognestad [33].

$$E_{cm} = 4700\sqrt{f_{cm}} \text{ (in MPa)} \quad (1)$$

where $E_{cm}$ is the modulus of elasticity, and $f_{cm}$ is compressive strength of concrete materials, respectively. Details of the CSRCWs are shown in Fig. 1.

To simulate the reinforced concrete wall and the composite steel–concrete elements, the ABAQUS software was employed. This software can provide a suitable nonlinear analysis for assessing the stress distribution and predicting the failure modes of composite elements. To consider the confining stress of steel tube on concrete, the sum of the confining stress from the tube and external confinement were assumed as proposed by researches [34,35].

To assess the stress distribution and crack propagation in concrete elements, three crack models are available in ABAQUS software: brittle cracking, concrete smeared cracking, and concrete damaged plasticity [36-38]. In the present study, the concrete damaged plasticity model was used. It can consider the both nonlinear compressive and tensile behaviors of concrete elements subjected to monotonic and dynamic loading [39]. The relationships between the stress and strain of concrete are given by Eqs. (2) and (3) for developing the concrete damaged plasticity model at tension and compression. Some properties, used by other researchers [39, 40], were employed to establish the concrete damaged plasticity model.

$$\sigma_t = (1-d_t)\, E_{cm}\, (\varepsilon_t - \varepsilon_t^{pl}) \qquad (2)$$

$$\sigma_c = (1-d_c)\, E_{cm}\, (\varepsilon_c - \varepsilon_c^{pl}) \qquad (3)$$

where $d_t$ and $d_c$ are the damage variables in tension and compression, respectively, and $\varepsilon_t^{pl}$ and $\varepsilon_c^{pl}$ are equivalent plastic strains in tension and compression, respectively, as shown in Fig. 2.

To develop the concrete damaged plasticity model, some parameters were considered. To consider the viscosity parameter ($\mu$) effects on the result of problem solution in software, the arranging $\mu$ for a few times is required. In this study, the $\mu$ parameter was selected for a very small number as reported by researchers [39,40]. The behavior of concrete subjected to compound stresses can be obtained from the dilation angle ($\psi$) parameter, which was assumed to be 31° based on Szczecina and Winnicki investigation [41]. To consider the yielding pattern for stress–strain curves of concrete, the modification coefficient of the deviatoric plane ($K_c$) was used in accordance with the Drucker-Prager yield criterion [42]. In this study, the $K_c$ was assumed for a value of 0.667 in concrete damaged plasticity model. The ratio of initial biaxial compressive yield stress to initial uniaxial compressive yield stress ($\sigma_{b0}/\sigma_{c0}$) was considered to be 1.16. The ratio of tensile to compressive strengths, defined as flow potential eccentricity ($\varepsilon$) was considered to be 0.1.

Shayanfar et al. [43] proposed Eqs. (4) and (5) for eliminating the dependence of the computed results on the finite element size. The model can be effectively employed to ensure reasonable accuracy.

$$\varepsilon_{tu} = 0.004\, e^{-0.008h} \qquad (\varepsilon_{tu} \geq \varepsilon_{cr}) \quad (4)$$

If $\varepsilon_{tu}$ is smaller than $\varepsilon_{cr}$, then

$$\varepsilon_{tu} = \varepsilon_{cr} \qquad (5)$$

where h is the width of the element in mm, and $\varepsilon_{tu}$ is the ultimate tensile strain of concrete.

Concerning the type of elements in ABAQUS software, three-dimensional (3D) hexahedral element, with 8 nodes and reduced integration (C3D8R) was used to simulate the concrete and rigid sections, similarly to what was employed by other researchers [36,38].

To assess the stress distribution and crack propagation in six specimens of the CSRCW, three types of steel materials with yield stresses of 300 MPa, 400 MPa and 500 MPa, and two grades of concrete with compressive strengths of 30 MPa and 40 MPa were considered in numerical modeling. Kheyroddin et al. [44] investigated the effect of high-strength reinforcement on structural behavior of moment-resisting frames. They reported that although high-strength reinforcements have economic benefits, they increase displacements and drifts, leading to an increase in steel quantity and dimensions

of members to compensate the rigidity

**Table 1.** The parameters of experimental specimens [30].

| Specimen ID | No and steel profile section | Encasement degree | Steel ratio | Axial load (kN) | Normalised axial level |
|---|---|---|---|---|---|
| CSRCW1 | 2-box section | Fully | 0.20 | 100 | 0.018 |
| CSRCW2 | 2-I-shaped section | Fully | 0.23 | 100 | 0.021 |
| CSRCW3 | 3-I-shaped section | Fully | 0.26 | 100 | 0.015 |
| CSRCW4 | 2-I-shaped section rotated by 90° | Fully | 0.20 | 100 | 0.016 |
| CSRCW5 | 2-I-shaped section | Partially | 0.22 | 100 | 0.015 |
| CSRCW6 | - | - | - | 100 | 0.016 |

**Table 2.** Properties of steel materials [30].

| Type | ID | Rebar diameter/steel thickness (mm) | $f_y$ (MPa) | $f_u$ (MPa) | $E_s$ (MPa) |
|---|---|---|---|---|---|
| Steel rebar | d8-1 | 8 | 483 | 616 | $2.09\times10^5$ |
| | d8-2 | 8 | 484 | 616 | $2.05\times10^5$ |
| | d8-3 | 8 | 471 | 617 | $2.01\times10^5$ |
| | d10-1 | 10 | 526 | 626 | $2.10\times10^5$ |
| | d10-2 | 10 | 559 | 624 | $2.15\times10^5$ |
| | d10-3 | 10 | 558 | 616 | $2.09\times10^5$ |
| I-shaped steel section | s-01 | 7 | 328 | 515 | $2.00\times10^5$ |
| | s-02 | 7 | 324 | 513 | $2.01\times10^5$ |
| | s-03 | 7 | 331 | 521 | $2.05\times10^5$ |

**Table 3.** Properties of the concrete elements [30].

| Specimen ID | No. of samples | $f_{cm}$ (MPa) | $E_{cm}$ (MPa) |
|---|---|---|---|
| CSRCW1 | 3 | 54.7 | 36628 |
| CSRCW2 | 3 | 46.0 | 34773 |
| CSRCW3 | 3 | 65.1 | 38591 |
| CSRCW4 | 3 | 62.0 | 38031 |
| CSRCW5 | 3 | 65.6 | 38680 |
| CSRCW6 | 3 | 63.5 | 38305 |

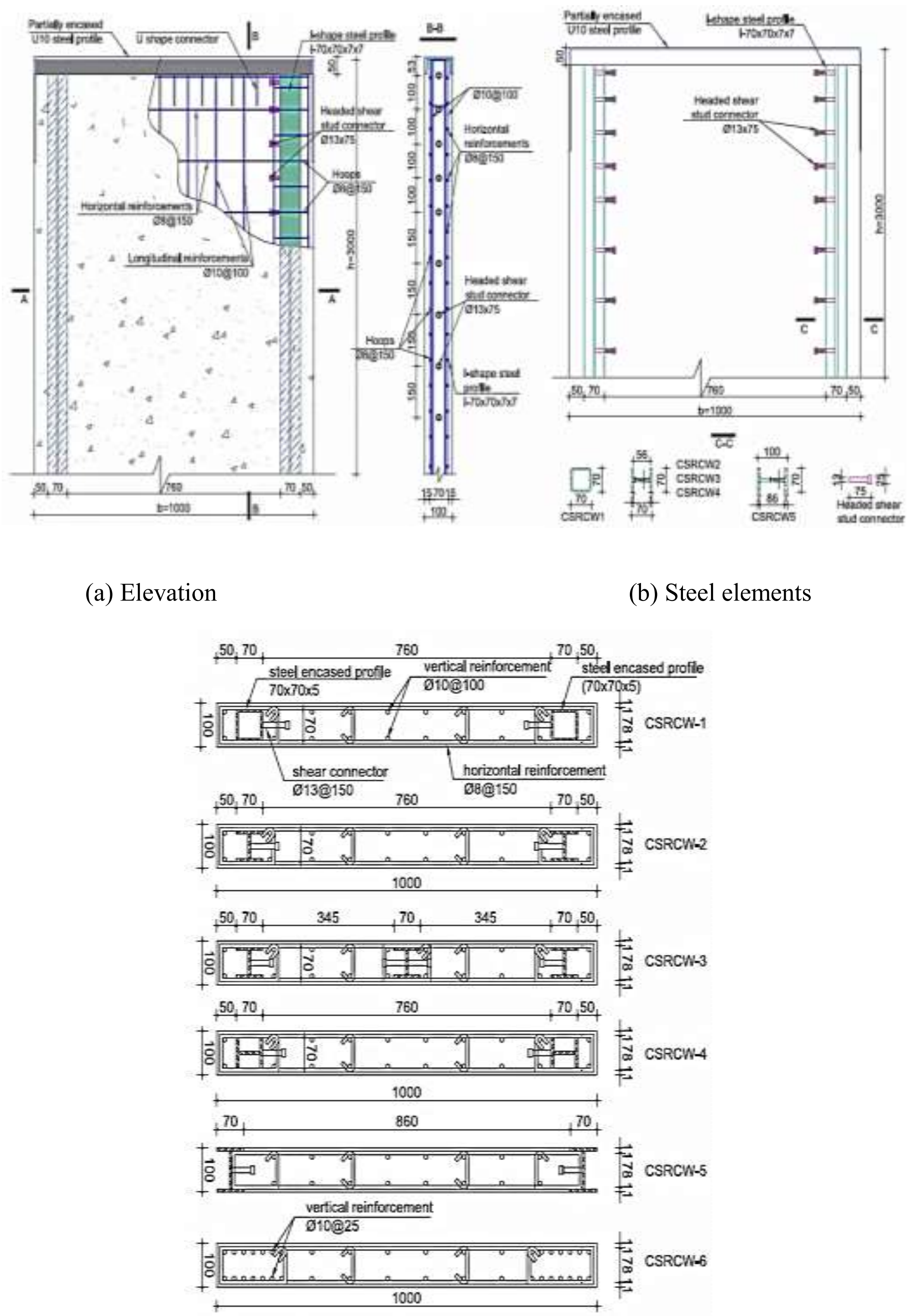


(a) Elevation (b) Steel elements

(c) A-A section

**Fig. 1.** Details of composite steel–concrete walls [30].

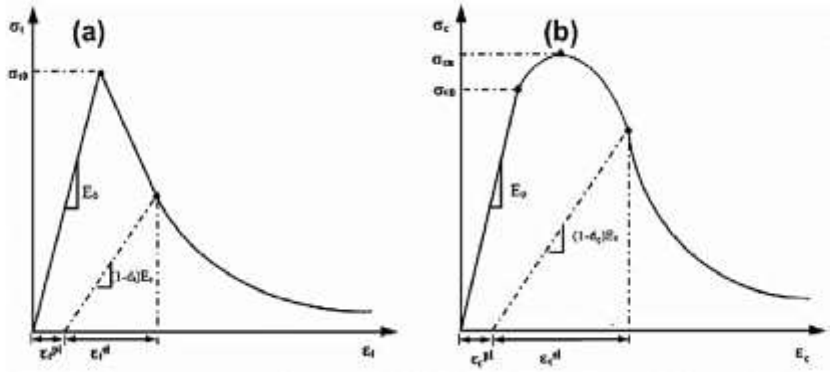

**Fig.2.** Concrete response subjected to uniaxial loading in tension (a) and compression (b) [45].

## 3. Verification of Finite Element Models

For verification, the numerical results of this study were compared to the experimental results of Dan et al. investigation [30]. According to the contour of compressive damage variable (DAMAGEC) (Fig. 3b), the crack propagation pattern approximately occurred at the base of CSRCW specimen, similar to what observed in the experimental results (Fig. 3a). Meanwhile, the general trends of CSRCW specimens in numerical studies were nearly the same obtained for experimental outputs given by Dan et al. [30] as shown in Figs. 4 and 5. Therefore, it can be stated that there was a good agreement between finite element analysis and experimental works. The critical forces for experimental specimens and numerical models were calculated as presented in Table 4.

**Table 4.** The difference between experimental and numerical results.

| Specimen ID | $P_{cr}$- Exp. (kN) | $P_{cr}$- Num. (kN) | Difference (%) |
|---|---|---|---|
| CSRCW1 | 255 | 280 | 9.80 |
| CSRCW2 | 247 | 268.62 | 8.75 |
| CSRCW3 | 278 | 295.41 | 6.26 |
| CSRCW4 | 246 | 271.55 | 10.38 |
| CSRCW5 | 266 | 290 | 9.02 |
| CSRCW6 | 192 | 207.17 | 7.90 |

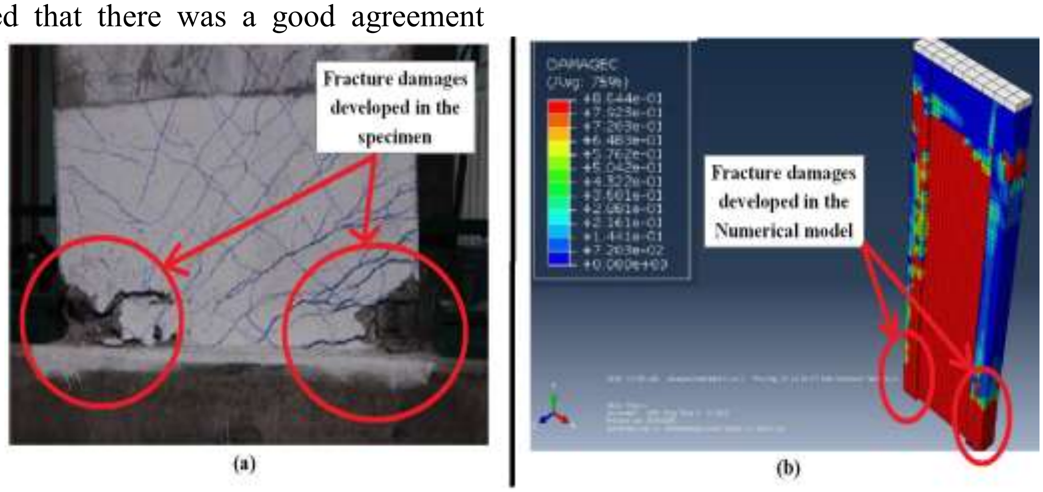


**Fig. 3.** Final failure appearance in the experimental specimen (a) and numerical model (b).

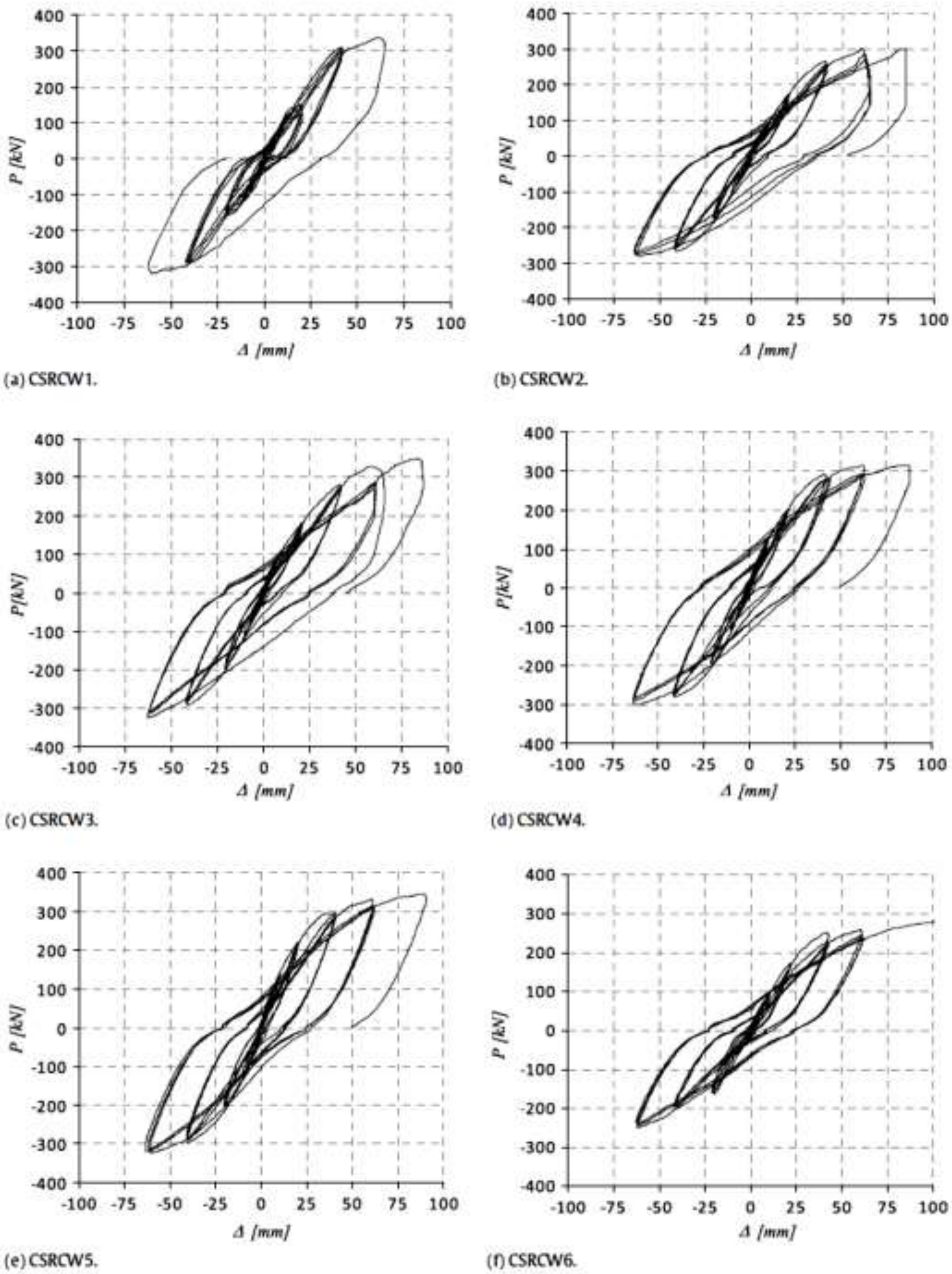


**Fig. 4.** Horizontal load versus lateral displacement (hysteretic curves) for experimental models: CSRCW1 (a); CSRCW2 (b); CSRCW3 (c); CSRCW4 (d); CSRCW5 (e); CSRCW6 (f) [30].

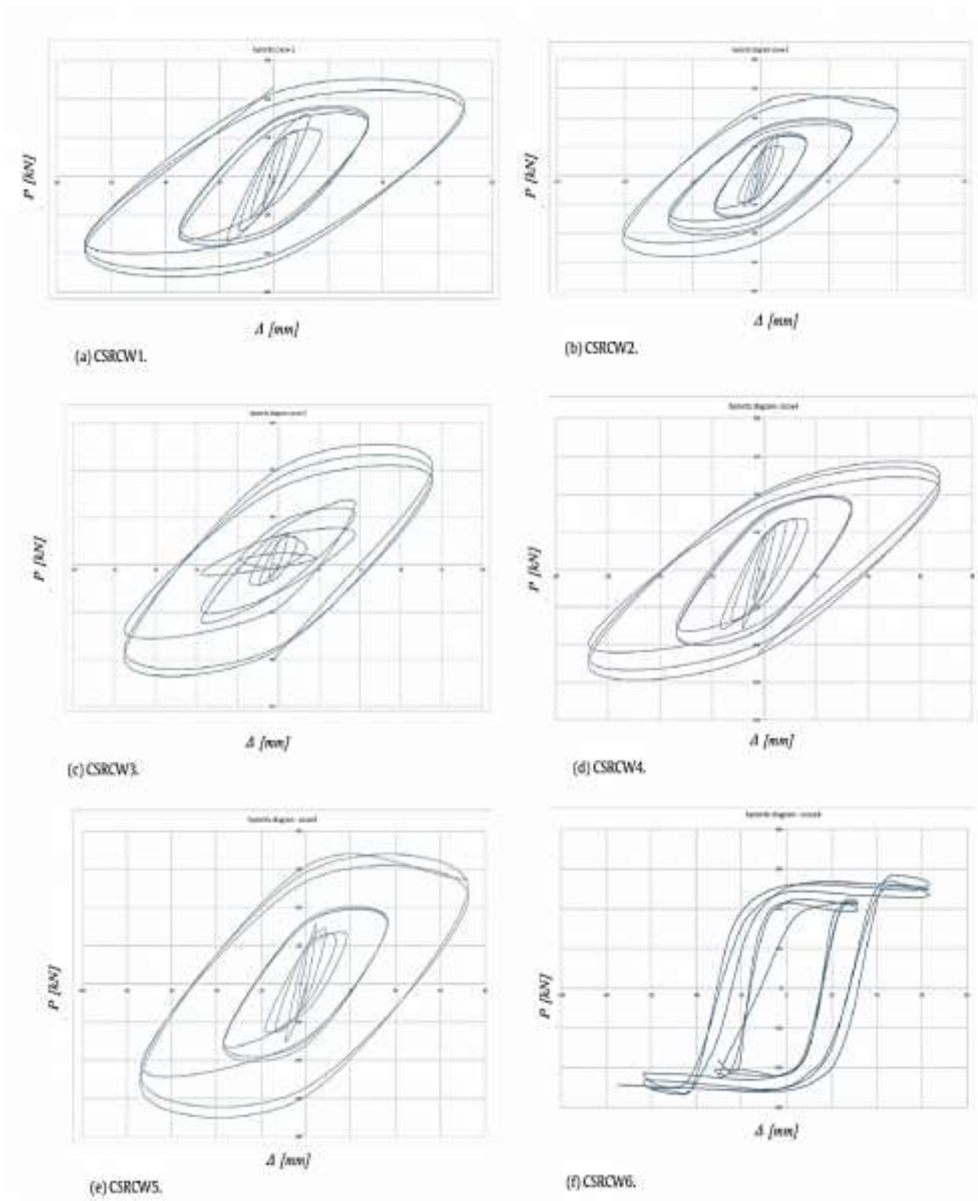


Fig. 5. Horizontal load versus lateral displacement (hysteretic curves) obtained for numerical models: CSRCW1 (a); CSRCW2 (b); CSRCW3 (c); CSRCW4 (d); CSRCW5 (e); CSRCW6 (f).

## 4. Results and discussions

In the present study, the performance of CSRCW specimens was numerically assessed for three types of steel materials with yield stresses of 300 MPa, 400 MPa and 500 MPa. In addition, two levels of compressive strength of concrete (30 MPa and 40 MPa) were introduced to numerical models to evaluate the lateral bearing capacity of the CSRCW.

As indicated in Fig. 6, ultimate strength of the CSRCW made with steel materials with the yield stress of 500 MPa was about 7.4% greater than that of 400 MPa. Meanwhile, the value for CSRCW made with steel materials with the yield stress of 500 MPa was on average about 10.3% more than that of 300 MPa. It can be inferred that by increasing the yield stress of steel materials, the composite shear walls were rehabilitated better.

Comparison of data on two CSRCW specimens made with compressive strength of 30 MPa and 40 MPa clarified that ultimate strength of the CSRCW made with concrete materials with the compressive strength of 40 MPa was on average about 7.7% higher than that of 30 MPa. Therefore, increasing compressive strength of concrete materials, the composite shear walls were rehabilitated better as expected.

Comparison of the results on CSRCW specimens made with different compressive strength of concrete materials and yield stresses of steel materials demonstrated that there is no remarkable difference between the results of CSRCW made with steel materials with the yield stress of 300 MPa and CSRCW made with concrete materials with compressive strength of 40 MPa. However, ultimate strength of the CSRCW made with steel materials with the yield stress of 500 MPa was on average about 7.1% higher than that made with concrete materials with the compressive strength of 40 MPa.

Generally, in most cases, CSRCW3 specimen appeared to have the highest lateral bearing capacity. For instance, the highest amount of ultimate strength was found to be 397.1 kN for CSRCW3-fy500. It seems that there was a good conjunction between steel materials and other components of composite shear walls. Meanwhile, the CSRCWs could absorb energy more by increasing the yield stress of steel materials particularly in boundary elements. Therefore, it can be concluded that the boundary element has a remarkable effect on increasing the lateral bearing capacity of developed numerical models.

On the other hands, the lowest ultimate strength was obtained for CSRCW6 specimen where there were no steel sections in boundary elements to improve the lateral bearing capacity of composite shear walls. It is worth mentioning that the rehabilitation of shear walls by means of RC columns as boundary elements in CSRCW6 could not efficiently increase the ultimate strength of wall. Apparently, this can be due to the fact that the tensile strength of concrete materials associated with steel sections was higher than that of concrete elements with no steel section in boundary elements.

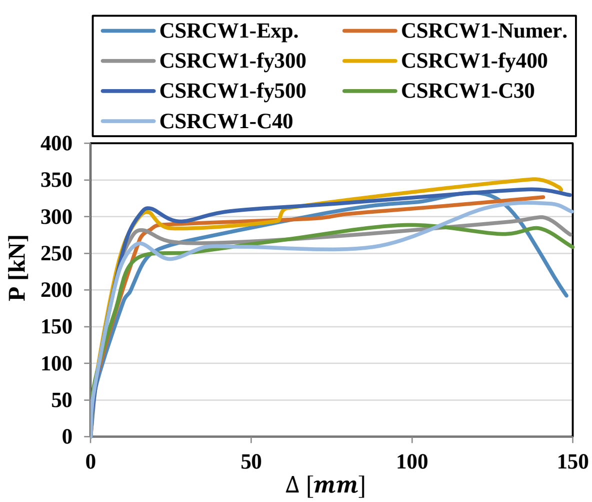


(a)

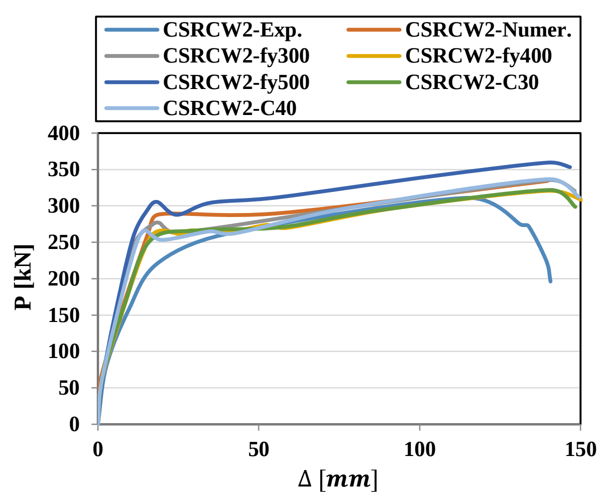


(b)

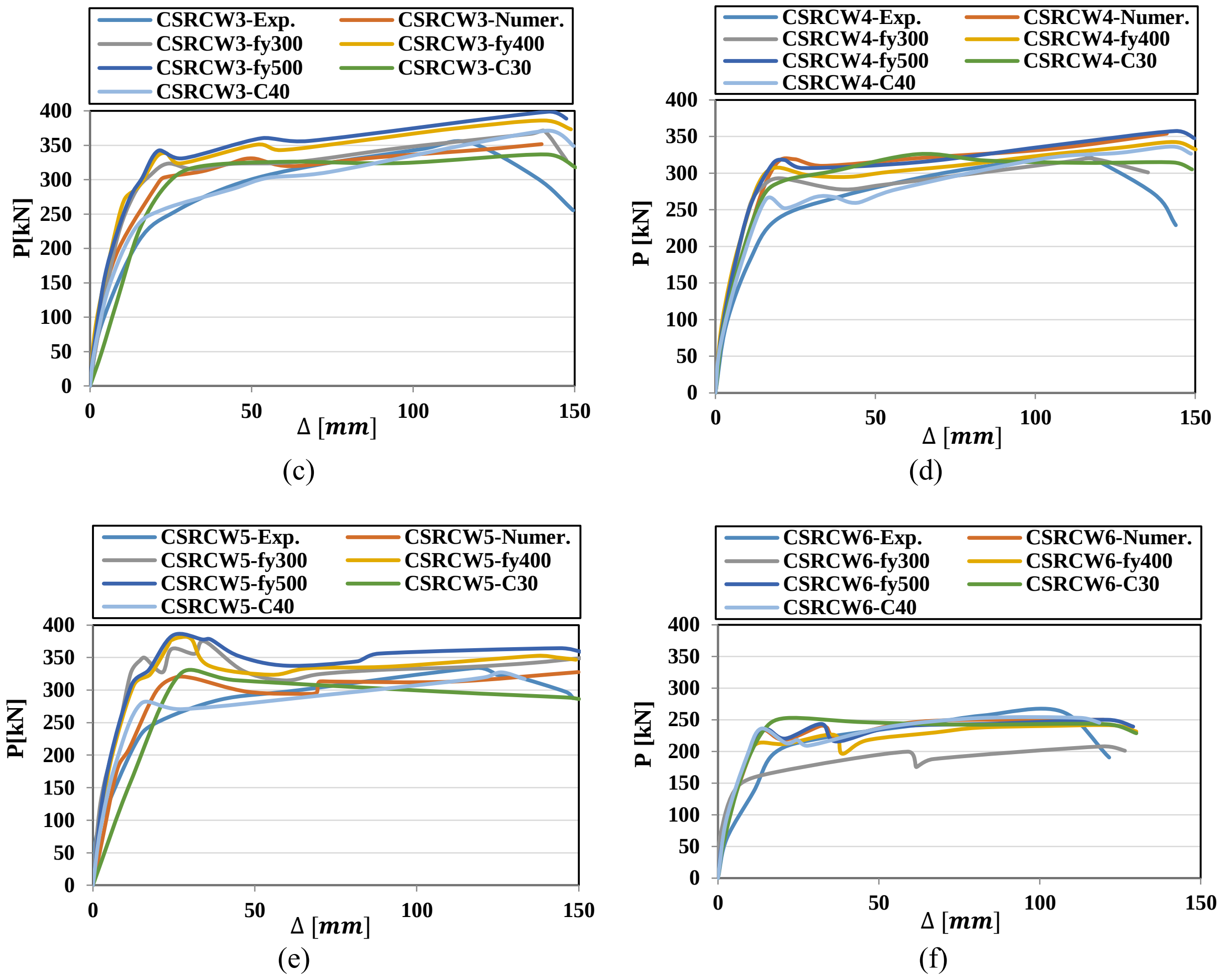


**Fig. 6.** Analytical P - Δ curves for CSRCW1 (a); CSRCW2 (b); CSRCW3 (c); CSRCW4 (d); CSRCW5 (e); CSRCW6 (f).

The stress distribution in steel elements for CSRCW1 and CSRCW3 specimens is shown in Fig. 7. The results demonstrated that the high stress for CSRCW1 specimen occurred in fracture zone at the base of shear walls, where it was equal to 586 MPa as indicated in Fig. 7(a). This value for CSRCW3 specimen was found to be 624 MPa by steel section in the middle of CSRCW as seen in the Fig. 7(b). Therefore, it can be concluded that the ratio of high stress obtained for CSRCW3 to CSRCW1 was 6.5%.

Another matter is that in the presence of steel section in the middle of shear wall (CSRCW3), the stress was distributed better throughout the shear walls, while most stresses in CSRCW1 specimen were concentrated at the base of the shear walls and it seems that by getting away from the base of the shear walls, different components of CSRCW1 could efficiently participate to bear the lateral loading without the presence steel section in the middle of CSRCW.

The assessment of the failure mode and stress distribution in Figs. 3 and 7 showed that there were some evidences for forming inelastic zone on CSRCWs, where the plastic deformations occurred in the composite walls. Therefore, it can be inferred that the behavior of these composite systems seems to be ductile. Thus the energy was efficiently dissipated between boundary elements and other components of shear walls.

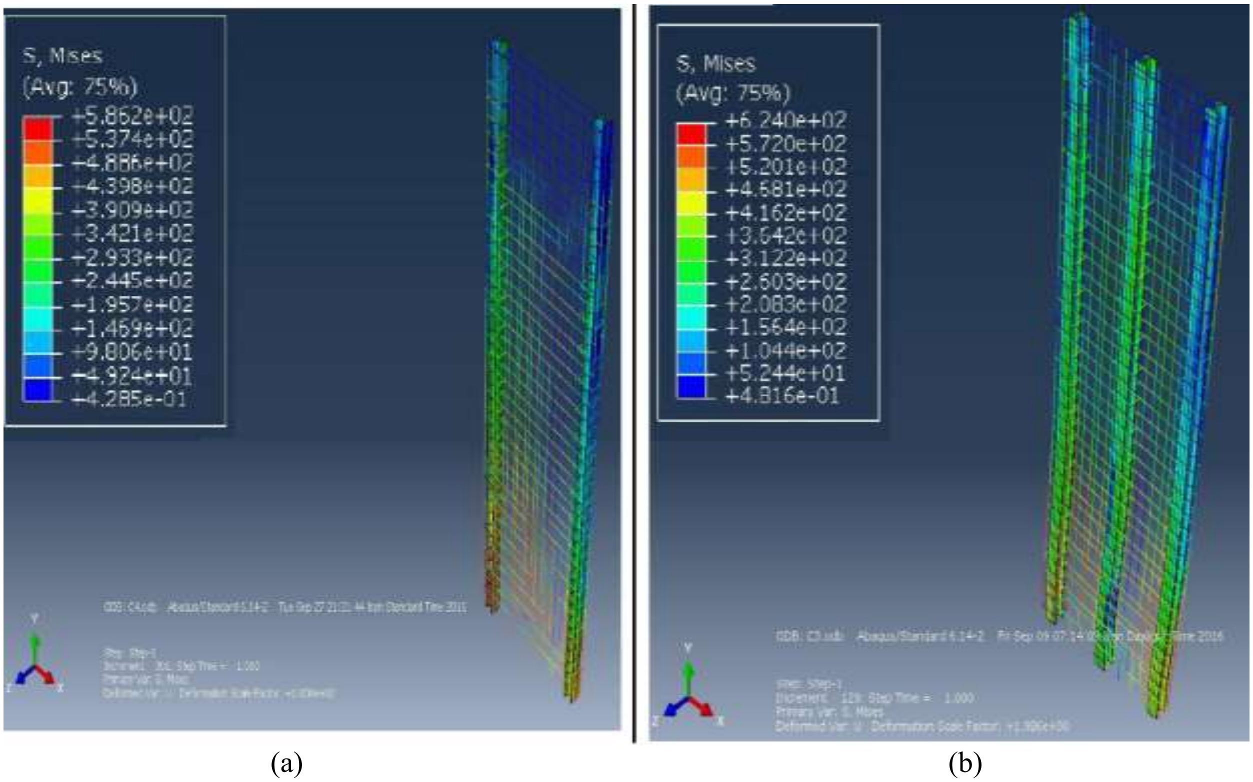


**Fig. 7.** Stress distribution of steel elements in CSRCW1 (a) and CSRCW3 (b)

## 5. Conclusions

In the present study, the behavior of CSRCWs with different types of steel and concrete materials was numerically assessed. Based on the numerical results, the following main conclusions can be drawn:

- The results showed that there was a fair agreement between the developed finite element models and experimental specimens. In addition, the results revealed that numerical models predicted the fracture zones similar to experimental observations and the contours of damage demonstrated that the fracture mechanisms of CSRCW specimens involved compressive damage evolution modes.
- By increasing the compressive strength of concrete materials and the yield stress of steel materials, the composite shear walls were rehabilitated better.
- Comparison of data on CSRCW specimens clarified that ultimate strength of the CSRCW made with steel materials with the yield stress of 500 MPa was on average about 7.1% higher than that made with concrete materials with the compressive strength of 40 MPa.
- According to the numerical results, CSRCW3-fy500 and CSRCW6-C30 specimens appeared to have the highest and lowest lateral bearing capacity, respectively. The highest amount of ultimate strength for the CSRCW was found to be 397.1 kN for CSRCW3-fy500 specimen.

- According to the numerical results, the ratio of high stress obtained for CSRCW3 to CSRCW1 was found to be 6.5%.
- Based on the numerical outputs, the presence of steel section in the middle of shear wall (CSRCW3) led to effectively distribute the stress throughout the shear wall.

## REFERENCES

[1] Viest, I.M., Colaco, J.P., Furlong, R.W., Griffis, L.G., Leon, R.T., Wyllie, L.A. (1997) “Composite construction: design for buildings” New York: McGraw-Hill.

[2] Kim, T., Foutch, D. (2007) “Application of FEMA methodology to RC shear wall buildings governed by flexure” Engineering Structures Vol. 29, pp. 2514–2522.

[3] Esmaeili, H., Kheyroddin, A., Kafi, M. A., Nikbakht, H. (2013) “Comparison of nonlinear behavior of steel moment frames accompanied with RC shear walls or steel bracings” The Structural Design of Tall and Special Buildings, Vol. 22, pp. 1062-1074.

[4] Ghods, S., Kheyroddin, A., Nazeryan, M., Mirtaheri S.M., Gholhaki, M. (2016) “Nonlinear behavior of connections in RCS frames with bracing and steel plate shear wall” Steel and Composite Structures, Vol. 22, pp. 915–935.

[5] Liao, F.Y., Han, L.H., Tao, Z. (2010) “Experimental behavior of RC shear walls framed with steel reinforced concrete (SRC) columns under cyclic loading” Steel and Composite Structures. In: Proceedings of the 4-th international conference, pp. 233–238.

[6] Esmaeili H., Kheyroddin A., Naderpour H. (2013) “Seismic behavior of steel moment resisting frames associated with RC shear walls” Iranian Journal of Science and Technology, Transaction B: Engineering, 37(C) pp. 395–407.

[7] Kheyroddin, A., Emami, E. (2016) “Shear walls” Semnan University Press, Semnan, Iran (in Persian), pp. 584-635.

[8] Kheyroddin, A., Naderpour, H. (2008). “Nonlinear finite element analysis of composite RC shear walls” Iranian Journal of Science and Technology, Transaction B: Engineering, Vol. 32, pp. 79-89.

[9] Kheyroddin A., Naderpour H. (2006) “Nonlinear finite element analysis of R/C shear walls retrofitted using externally bonded steel plates and FRP sheets” In: 1st International structural specialty conference, Calgary-Canada; p. ST- 093-1-10.

[10] Kazemi, M., Kafi, M. A., Hajforoush, M., Kheyroddin, A. (2019) “Cyclic behaviour of steel ring filled with compressive plastic or concrete, installed in the concentric bracing system” Asian Journal of Civil Engineering, pp. 1-11.

[11] Kazemi, M., Hajforoush, M., Khakpour Talebi, P., Daneshfar, M., Shokrgozar, A., Jahandari, S., Saberian, M., Li, J. (2020) “In-situ strength estimation of polypropylene fibre reinforced recycled aggregate concrete using Schmidt rebound hammer and point load test” Journal of Sustainable Cement Based Materials pp. 1-18.

[12] Gholhaki, M., Kheyroddin, A., Hajforoush, M., Kazemi, M. (2018) “An investigation on the fresh and hardened properties of self-compacting concrete incorporating magnetic water with various pozzolanic materials” Construction and Building Materials Vol. 158, pp. 173-180.

[13] Hajforoush, M., Madandoust, R., Kazemi, M. (2019) “Effects of simultaneous utilization of natural zeolite and magnetic

water on engineering properties of self-compacting concrete" Asian Journal of Civil Engineering, Vol. 20 (2), pp. 289–300.

[14] Guan, M., Liu, W., Lai, M., Du, H., Cui, J., Gan, Y. (2019) "Seismic behaviour of innovative composite walls with high-strength manufactured sand concrete" Engineering Structures Vol.195, pp. 182–199.

[15] Tupper, B. (1999) "Seismic response of reinforced concrete walls with steel boundary elements" Thesis for the degree of Master of Engineering. Mc Gill University; Montreal, Canada.

[16] Zhao, W., Guo, Q., Huang, Z., Tan, L., Chen, J., Ye, Y. (2016) "Hysteretic model for steel–concrete composite shear walls subjected to in-plane cyclic loading" Engineering Structures, Vol. 106, pp. 461–470.

[17] Zhang, H., Liu, H., Li, G., Ning, X. (2019). "Seismic performance of encased steel plate-reinforced gangue concrete composite shear walls" Structural Engineering, pp. 1-14.

[18] Teng Huang, S., Sheng Huang, Y., He, A., Lin Tang, X., Jun Chen, Q., Liu, X., Cai, J. (2018). "Experimental study on seismic behaviour of an innovative composite shear wall" Journal of Constructional Steel Research. Vol. 148, pp. 165–179.

[19] Rassouli, B., Shafaei, S., Ayazi, A., Farahbod, F. (2016) "Experimental and numerical study on steel-concrete composite shear wall using light-weight concrete" Journal of Constructional Steel Research Vol.126, pp. 117-128.

[20] Kheyroddin, A., Mirza, M.S. (1995) "Flexural rigidity of reinforced concrete beams." In Canadian Society for Civil Engineering Annual Conference Proceedings, pp. 1-3.

[21] Kheyroddin, A. (1996) "Nonlinear finite element analysis of flexure-dominant reinforced concrete structures." Ph.D. Thesis, Department of Civil Engineering and Applied Mechanics, McGill University, Montreal, Canada, 290p.

[22] Ayazi A, Shafaei S. (2019) "Steel–concrete composite shear walls using precast high performance fiber reinforced concrete panels" The Structural Design of Tall and Special Buildings, 1617.

[23] Dan, D., Stoian, V., Fabian, A. (2009) "Numerical analysis of composite steel concrete structural shear walls with steel encased profiles" Buletinul Ştiinţific al Universităţii Gheorghe Asachi din Iaşi, BDI B, Vol. LIX, pp. 21 – 32.

[24] Stoian, V., Dan, D., Fabian, A. (2011) "Composite shear walls with encased profiles, new solution for buildings placed in seismic area" Acta Tech Napocensis Civ Eng Architect, Vol. 54, pp. 6–12.

[25] Sun, G., Gu, Q., Li, Q., Fang, Y. (2018) "Experimental and numerical study on the hysteretic behavior of composite partially restrained steel frame-reinforced concrete infill walls with vertical slits" Bulletin of Earthquake Engineering, Vol. 16, pp. 1245-1272.

[26] Saari, W.K., Hajjar, F.J., Schultz, A.E., Shield, C.K. (2004) "Behavior of shear studs in steel frames with reinforced concrete infill walls" Journal of Constructional Steel Research, Vol. 60, pp. 1453–1480.

[27] Hossain, A.K.M., Wright, H.D. (2004) "Experimental and theoretical behavior of composite waling under in-plane shear" Journal of Constructional Steel Research, Vol. 61, pp. 59–83.

[28] Tong, X.T., Hajar, J.F. (2005) "Schultz AE, Shield CK. Cyclic behavior of steel frame structures with composite reinforced concrete infill walls and partially restrained connections" Journal of Constructional Steel Research, Vol.61, pp. 531–52.

[29] Rahnavard, R., Hassanipour, A., Mounesi, A. (2016) "Numerical study on important parameters of composite steel-concrete

shear walls" Journal of Constructional Steel Research, Vol. 121 pp. 441–456.

[30] Dan, D., Fabian, A., Stoian, V. (2011) Theoretical and experimental study on composite steel– concrete shear walls with vertical steel encased profiles Original Research Article" Journal of Constructional Steel Research, Vol. 67, pp. 800–813.

[31] Astaneh, A.A. (2002) "Seismic behavior and design of composite steel plate shear walls.Steel tips" University of California: Berkeley.

[32] Epackachi, S., Whittaker, A., Varma, A. H., and Kurt, E. (2015) "Finite element modeling of steel-plate concrete composite wall piers" Engineering Structures, Vol. 100, pp. 369–384.

[33] Hognestad, E. A. (1951) "study on combined bending and axial load in reinforced concrete members" Univ. of Illinois at Urbana-Champaign, IL, pp. 43–46. Bulletin Series No. 399.

[34] Lai, M.H., Ho, J.C.M. (2016) "A theoretical axial stress-strain model for circular concrete-filled-steel-tube columns" Engineering Structures, Vol. 125, pp. 124-143.

[35] Lai, M.H., Liang, Y.W. Wang, Q. Ren, F.M. Chen, Ho, M.T. J.C.M. (2020) "A stress-path dependent stress-strain model for FRP-confined concrete" Engineering Structures, Vol. 203, 109824.

[36] Hibbitt, D., Karlsson, B., Sorensen, P. (2011) "ABAQUS Standard User's Manual" Version (6.11-3).

[37] Madandoust, R., Bazkiyaei, Z.F.Z., Kazemi, M. (2018) "Factor influencing point load tests on concrete" Asian Journal of Civil Engineering, 19(8), 937-947.

[38] Madandoust, R., Kazemi, M., Moghadam, S.Y. (2017) "Analytical study on tensile strength of concrete" Romanian Journal of Materials, Vol. 47, pp. 204–209.

[39] Madandoust, R., Kazemi, M. (2017) "Numerical analysis of break-off test method on concrete" Construction and Building Materials, Vol. 151, pp. 487–493.

[40] Moghadam, S.Y., Madandoust, R., Ranjbar, M.M., Kazemi, M. (2017) "Analytical study on the behavior of corrosion damaged reinforced concrete beams strengthen with FRP" Romanian Journal of Materials, Vol. 47, pp. 514 – 521.

[41] Szczecina M, Winnicki A. (2015) "Calibration of the CDP model parameters in Abaqus" Incheon, Korea: World Congress on Advances in Structural Engineering and Mechanics.

[42] Drucker DC, Prager W. (1952) "Soil mechanics and plastic analysis or limit design" Q Appl Math, Vol. 10, pp.157–65.

[43] Shayanfar, M.A., Kheyroddin, A., Mirza, M.S. (1997) "Element size effects in nonlinear analysis of reinforced concrete members" Computers & Structures, 62(2), pp.339-352.

[44] Kheyroddin, A., Arshadi, H., Binaipur, F. (2017) "An overview of the effects of high-strength reinforcement (HSR) on the intermediate moment-resisting frames" AUT Journal Civil Engineering, 1(2), pp. 177-188.

[45] Kazemi, M., Li, J., Lahouti Harehdashta, S., Yousefiehc, N., Jahandarid, S., Saberianb, M. (2020) "Non-linear behaviour of concrete beams reinforced with GFRP and CFRP bars grouted in sleeves" Structures Vol. 23 pp. 87–102.